Acoustic Characteristics of PMMA in the Steady Stress–Strain State Investigated by Coherent Brillouin Scattering Method

T. SAKURAI, T. MATSUOKA, S. KODA, H. NOMURA

Department of Molecular Design and Engineering, Graduate School of Engineering, Nagoya University, Chikusa-ku, Nagoya 464-8603, Japan

Received 1 July 1999; accepted 14 September 1999

ABSTRACT: The acoustic properties of PMMA poly(methyl methacrylate) deformed by tensile stress were investigated by the coherent Brillouin scattering method. The ultrasonic velocities of PMMA in steady stress–strain states were measured in the frequency range of 100 MHz to 1 GHz. The ultrasonic velocities decreased with increasing strain, and the ratio of the decrease increased with increasing strain rate. This result indicates that the crazing residues still remain in the steady stress–strain states, and the amount of the residues depends upon the strain rate. The velocity dispersion was observed around 400 MHz for virgin and deformed PMMA and reproduced with a single relaxation process. The relaxation process is assigned to the γ-relaxation according to the dispersion map for methyl group relaxation in PMMA. The relaxation frequency and strength were independent of the applied stress and strain. The viscoelastic and plastic deformations have little effect on the γ-relaxation. © 2000 John Wiley & Sons, Inc. J Appl Polym Sci 76: 978–986, 2000

Key words: steady stress–strain state; strain rate; poly(methyl methacrylate); γ-relaxation; coherent Brillouin scattering

INTRODUCTION

Polymers are used extensively as industrial materials, because they have a number of advantages, such as ease of processing, low density, and various unique properties as compared to other industrial materials. In engineering applications, they are placed under mechanical stress. Thus, mechanical properties during deformation processes attract much attention.

Ultrasonic velocity measurement is the most useful method to investigate such mechanical properties as elasticity and compressibility.[1–4] During the deformation process, these mechanical properties are affected by changes in the molecular orientation and packing state, and ultrasonic propagation in the materials is quite sensitive to their changes. Yap et al.[5] studied the acoustic properties of PMMA poly(methyl methacrylate) under uniaxial tensile stress using the Brillouin scattering method and reported the strain dependence of the ultrasonic velocities. Kawabe et al.[6] observed the strain dependence of the ultrasonic velocities by scanning acoustic microscopy and stated that the "embryo" of crazing produced in the deformation process before crazing affected the acoustic properties of PMMA. However, the strain rate dependence of the acoustic properties remains to be well understood. For amorphous polymeric materials, it is well known that stress increases nonlinearly with increasing strain, and the stress–strain curve depends upon

Correspondence to: T. Sakurai.

Journal of Applied Polymer Science, Vol. 76, 978–986 (2000)
© 2000 John Wiley & Sons, Inc.

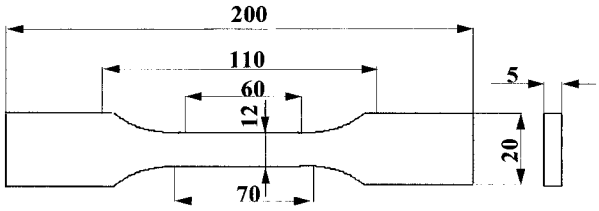

Figure 1 Dimensions of specimen (mm).

the strain rate.[7] Strain rate dependence is also observed for creep and stress relaxation. Thus, the mechanical properties under uniaxial tensile stress will be affected by the strain rate. Plastic deformation, such as the embryo of crazing, may cause strain rate dependence of the acoustic properties.

Recently, a new phase-coherent light-scattering method, the coherent Brillouin scattering (COBS), was developed by Tanaka et al.[8] This method is a light-scattering technique in which the light is scattered by optically generated coherent phonons instead of thermally excited phonons. In this method, the scattered light is detected as a heterodyne signal in the lock-in detection. The COBS method realizes both high resolution and high signal-to-noise ratio (SNR) at the same time, both of which are required for high-precision spectroscopy. To apply the COBS method to the study of the acoustic properties of condensed matter, we constructed an experimental system in which the intensity of the coherent phonons was enhanced by using high-power frequency-tunable lasers, and we succeeded in measuring the ultrasonic velocities of several organic liquids in the frequency range of several hundred MHz to GHz.[9,10] The COBS method is applicable for studying the acoustic properties of condensed matter in an external stress field, and it is useful for measuring the ultrasonic velocity of uniaxially stretched specimens with high accuracy.

This article deals with the acoustic properties of PMMA deformed by the tensile stress. Emphasis is placed on the changes of the ultrasonic velocities caused by the strain and strain rate in the frequency range of 100 MHz to 1 GHz. The velocity dispersions observed for virgin and deformed PMMA are also discussed.

EXPERIMENTAL

Sample

Commercially available PMMA sheets of 5-mm in thickness were used. The specimens were cut from the sheets and shaped to their dimensions according to ASTM D638, as shown in Figure 1.

Experimental Condition

The deformation processes of the PMMA specimen are schematically illustrated in Figure 2. The specimen was uniaxially stretched with Shimadzu AG-25TE tester in the path (1), and the following two states were studied.

1. State A: On the stress–strain curve shown in Figure 2, the stress relaxes at a constant strain, and then reaches a steady-state value, σ_A following the process (2) in Figure 2(a). The steady stress–strain state is kept in a state A.
2. State B: The steady-state stress, σ_A is released in the state A. The strain diminishes along path (4), as shown in Figure 2(b). The reversible deformation of the specimen recovers to a state B.

The specimen in states A and B are called "PMMA in the state A" and "PMMA in the state B," respectively. In path (1), the specimen was deformed at the strain rate of 0.1, 0.5, and 1.0 mm/min at room temperature. To attain the states at various strains on the stress–strain curve, the stress applied to the specimen was changed from 20 to 70 MPa.

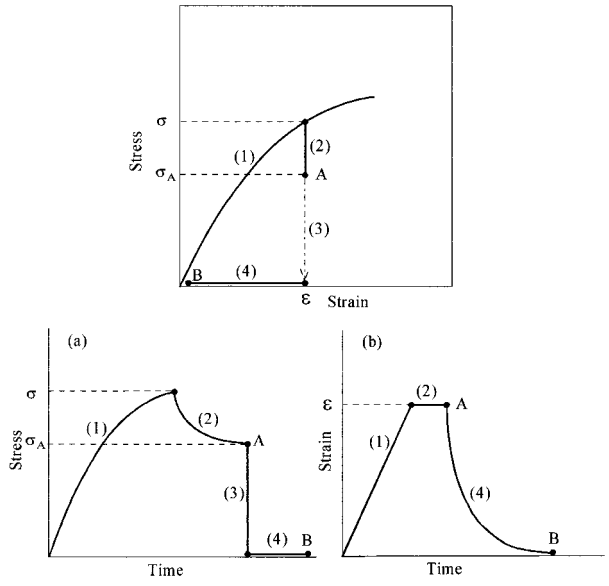

Figure 2 Schematic illustration of the deformation process.

Ultrasonic Velocity and Density Measurements

The detailed description and procedures of the COBS method for the ultrasonic velocity measurement have been given in the literature,[8] however, only a brief outline is given here. We used two frequency-tunable lasers with a power of 200 mW (Model 140-0532-200, Lightwave Electronics; single axial mode, continuous wave output, frequency-doubled green Nd:YAG laser) in our COBS apparatus.[9] In the COBS measurement, the complex resonance spectra of the laser-induced coherent phonons are measured as a function of beat frequency of two laser beams. The ultrasonic velocity is calculated from the following equation.

$$c = \omega/k_p \qquad k_p = 2q \sin(\theta/2) \tag{1}$$

where ω is the frequency of phonon, k_p the wave number of phonon, q the wave number of the laser light, and θ the crossing angle of two laser beams. Experimental errors of the ultrasonic velocities were within $\pm 0.1\%$.

The ultrasonic velocity measurement system of PMMA in the state A is indicated in Figure 3. The X, Y, and Z axes are selected, as shown by the arrows in Figure 3. When two laser beams are located in the X–Y plane, the coherent phonons excited in the materials propagate along the Y-axis. The Y and Z axes correspond to the "perpendicular" and "parallel" directions to the loading direction, respectively. The ultrasonic velocities of PMMA in the state A were measured in the direction perpendicular to the loading direction. The ultrasonic velocities of PMMA in the state B were measured in the directions both perpendicular and parallel to the loading direction. The ultrasonic velocities of virgin PMMA and PMMA in state B were measured at 5 MHz using the time-to-amplitude converter method.[1]

Densities of the specimens were measured using the pycnometer. Experimental errors of density data were $\pm 0.5\%$. All measurements were carried out at 294 $\pm$ 0.2 K.

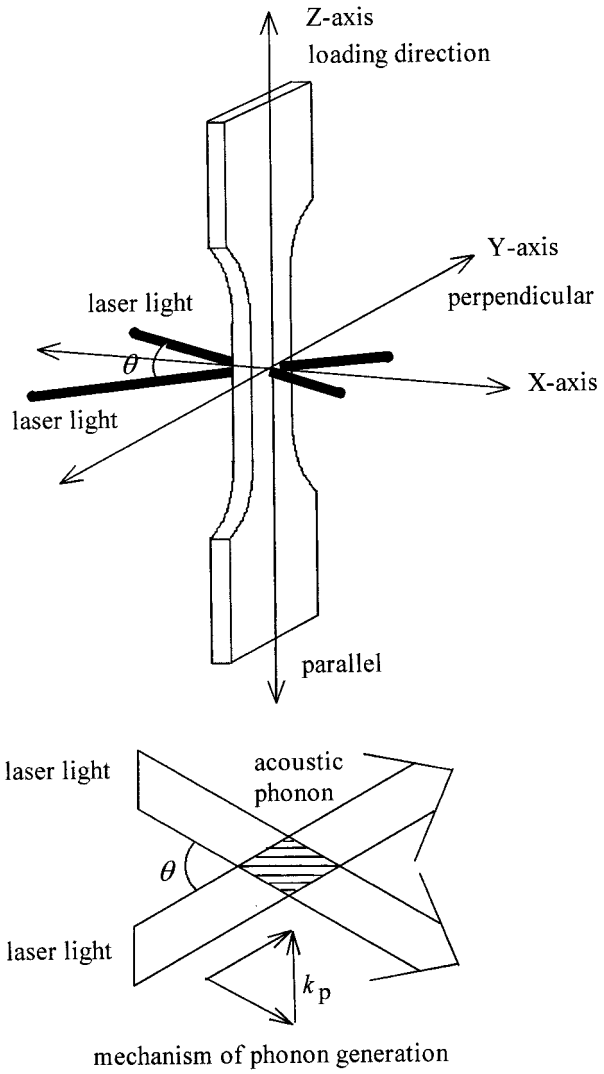

Figure 3 Ultrasonic measurement system in state A.

RESULTS

Stress–Strain, Stress Relaxation, and Creep Recovery Curves

Figure 4 shows stress–strain curves of PMMA at different strain rates corresponding to path (1) in Figure 2. The nonlinear deformation is observed for PMMA, and the stress–strain curves depend upon the strain rate. These experimental results are in good agreement with those reported by Sadd and Morris.[11] The arrows in Figure 4 indicate the breaking points. As seen in Figure 4, the strain at breaking point decreases with increasing strain rate, but the stress at breaking point increases with increasing strain rate.

The stress relaxation process (2) in Figure 2, while keeping the strain a constant, is shown in Figure 5. In the short time region, the stress relaxes very sharply, then gradually decreases to the steady-state stress, σ_A. The σ_A observed for all the experimental conditions are shown by the filled symbols in Figure 4 as a function of strain.

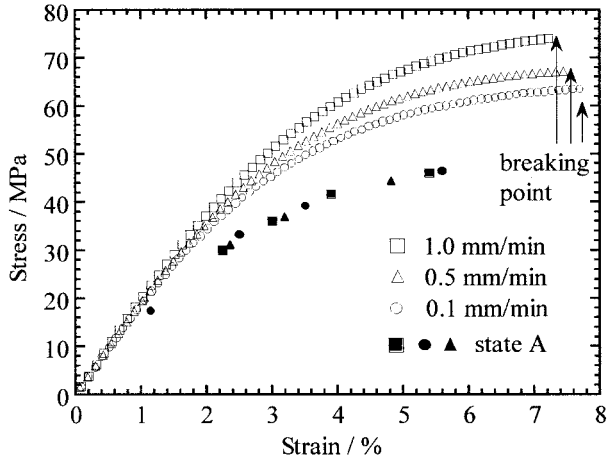

Figure 4 Stress–strain curves of PMMA at different strain rates. The filled circles represent the stress–strain relationship of PMMA in state A.

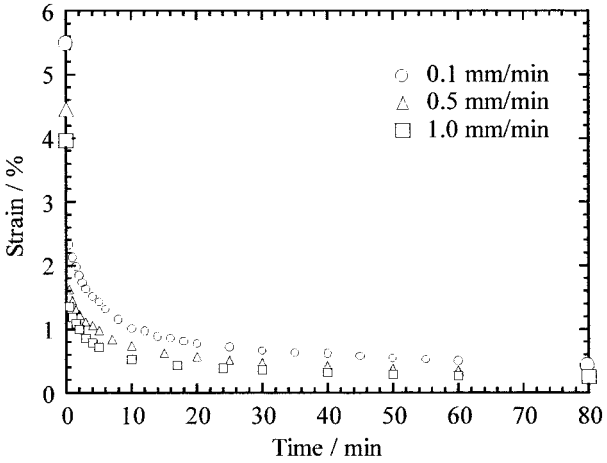

Figure 6 Creep recovery curves observed in path (4). Tensile stress of 60 MPa at different strain rates is applied in path (1).

The value of σ_A depends upon the strain, but is independent of the strain rate of the deformation. Figure 6 represents the creep recovery process (4) as shown in Figure 2. The strain relaxes to a steady-state B in Figure 2. The strain of PMMA in state B was less than 0.5% for all experimental conditions.

Ultrasonic Velocity and Density Measurements

Figure 7 shows the real and imaginary parts of complex resonance spectra of virgin PMMA observed around 470 MHz. The ultrasonic velocity calculated using eq. (1) was 2780 m/s.[12] The strain dependence of the ultrasonic velocities measured is shown in Figure 8. For PMMA in the state A, the ultrasonic velocities decrease linearly with increasing strain, and the slope of the line increases with increasing strain rate. The ultrasonic velocities of PMMA in state B are also plotted as a function of strain at the moment of releasing the stress. A similar linear relation was also observed in state B, but their slopes were steeper than those in state A.

The ultrasonic velocity measurements in state A are carried out for the specimen held on the tensile mechanical tester. Thus, it is difficult to measure the directional dependence of the ultrasonic velocities in state A. On the other hand, the directional dependence of the ultrasonic velocities

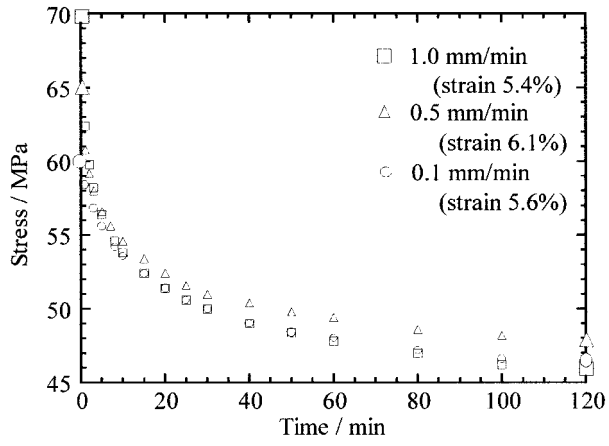

Figure 5 Time dependence of the stress relaxation observed in path (2).

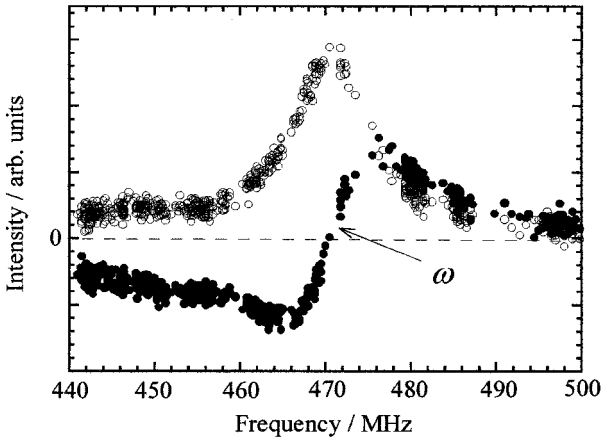

Figure 7 Complex resonance spectra of virgin PMMA around 470 MHz obtained by the COBS method. The filled and open circles are real and imaginary parts of spectra, respectively.

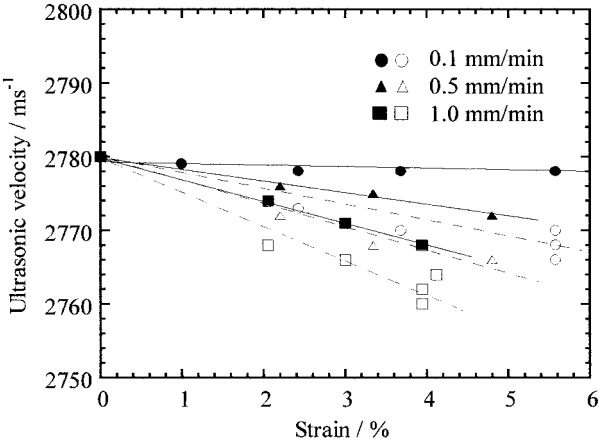

Figure 8 Strain dependence of the ultrasonic velocities at different strain rates. The filled and open symbols indicate the values measured in the states A and B, respectively.

can be measured for the specimen in state B, because the specimen can be taken off the mechanical tester. However, no directional anisotropy of the ultrasonic velocities was observed for PMMA in state B.

The ultrasonic velocities as a function of frequency are shown in Figure 9. The velocity dispersion is observed for virgin and deformed PMMA. Solid curves are those fitted with a single relaxation equation described as follows:

$$c^2(f) = c_0^2 + (c_\infty^2 - c_0^2)\left[\frac{(f/fr)^2}{1 + (f/fr)^2}\right] \tag{2}$$

where f is the frequency, fr the relaxation frequency, subscripts 0 and ∞ refer to the low- and high-frequency limiting values, respectively. The relaxation strength is given as follows:

$$\varepsilon = (c_\infty^2 - c_0^2)/c_\infty^2 \tag{3}$$

The observed relaxation strength was 0.028, regardless of the experimental conditions. The relaxation frequency is 410 MHz, as shown by the arrow in Figure 9.

The density measurements were carried out for virgin PMMA and PMMA in state B. The density of virgin PMMA was 1.18_5 g/cm^3, with accuracy of $\pm 0.5\%$. The density of PMMA in state B was around 1.18_2 g/cm^3 for all experimental conditions in path (1) and was in agreement with that of virgin PMMA.

DISCUSSION

It has been recognized that the large deformation of brittle polymeric materials such as PMMA consists of two parts: one is viscoelastic, and the other is the plastic deformation.[11,13–15] In this case, the tensile stress–strain relationship is linear at low strain region, followed by a region of non-linear behavior, and finally extends to a region of perfectly plastic flow. The stress for the large deformation can be written as

$$\sigma = \sigma_{\text{elastic}} + \sigma_{\text{plastic}} \tag{4}$$

where the first term is dominant in the linear deformation region, and the second term describes the stress in the strain levels exceeding the linear behavior region. As a first and rough approximation, we applied the stress–strain relation based on the three parameter viscoelastic solid model[16] with a single relaxation time for the first term on the right-hand side of eq. (4). The stress–strain equation in the case of constant strain rate loading is described as follows[17]:

$$\sigma_{\text{elastic}}(\varepsilon) = \frac{E_1 E_2}{E_1 + E_2}\,\varepsilon + \frac{E_1^2 T\tau}{E_1 + E_2} \times \left[1 - \exp\left(-\frac{\varepsilon}{T\tau}\right)\right] \quad (0 \le \varepsilon \le \varepsilon_0) \tag{5}$$

where E is the elastic modulus, T the strain rate, and τ the relaxation time. As for the nonlinear

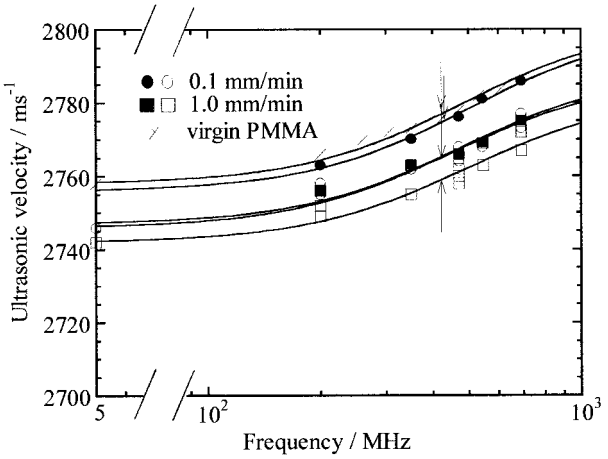

Figure 9 Ultrasonic velocities as a function of frequency. The solid curves are those fitted to eq. (2). The arrow represents the relaxation frequency. Tensile stress of 60 MPa at different strain rates is applied in path (1).

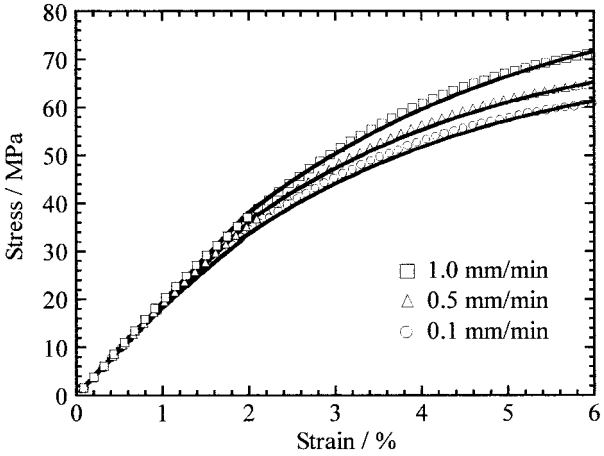

Figure 10 Results of the analyses of the stress–strain curves. Solid curves are those fitted to eq. (4).

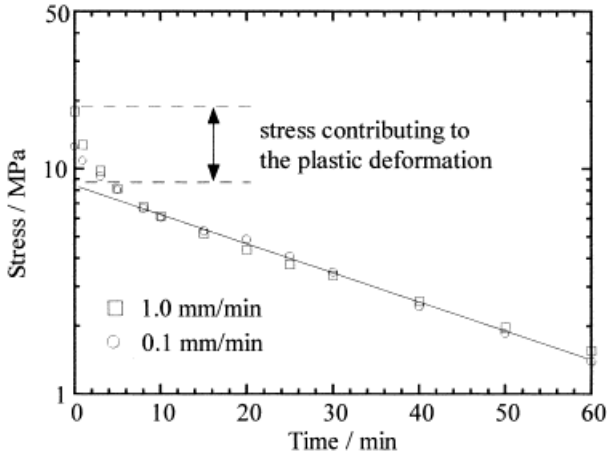

Figure 11 Semilogarithmic plots of the stress relaxation. The solid line are those fitted to eq. (7).

relations between the stress and strain attributable to plastic deformation, we assumed the mechanical model of Bingham type.[11]

$$\sigma_{\text{plastic}}(\varepsilon) = Y + \eta T\left\{1 - \exp\left[-\frac{E_1}{\eta T}(\varepsilon - \varepsilon_0)\right]\right\} \quad (\varepsilon \geq \varepsilon_0) \quad (6)$$

where η is the viscosity, and $Y = \sigma_{\text{elastic}}(\varepsilon_0)$. The stress–strain curves calculated by eq. (4) are shown by the solid curves of Figure 10. The curves are in agreement with our experimental data for PMMA. Our experimental results for large deformation of PMMA support the above deformation model.

The plastic deformation also affects the stress and creep relaxation processes.[7] The stress relaxation and creep recovery processes, as well as the stress–strain relationship, are caused by the viscoelastic and plastic deformations. Figures 11 and 12 show the semilogarithmic plots of the stress relaxation and creep recovery curves in paths (2) and (4) shown in Figure 2. As seen in Figures 11 and 12, the stress relaxation and creep recovery consist of two relaxation processes; one is the relaxation process observed in the shorter time region, and the other is the relaxation process in which the relationship between time and ln σ is linear. The plastic deformation is associated with the relaxation process in the shorter time region.[7] The stress relaxation and creep recovery shown by the solid lines in Figures 11 and 12 are represented by the three parameter viscoelastic solid model as follows.[16]

$$\sigma_{\text{elastic}}(t) = \frac{E_1E_2}{E_1 + E_2}\varepsilon + \left(\sigma_{t\to 0} - \frac{E_1E_2}{E_1 + E_2}\varepsilon\right)\exp\left(-\frac{t}{\tau}\right) \quad (7)$$

$$\varepsilon_{\text{elastic}}(t) = \frac{E_1 + E_2}{E_1E_2}Y_1\left[1 - \left(1 - \frac{E_2}{E_1 + E_2}\right)\exp\left(-\frac{t}{\tau}\right)\right] \quad (8)$$

where Y_1 is the parameter for representing the strain after creep recovery. We estimated the stress or strain contributing to the plastic deformation by subtracting the extrapolated values at $t \to 0$ from the experimental ones at $t = 0$.

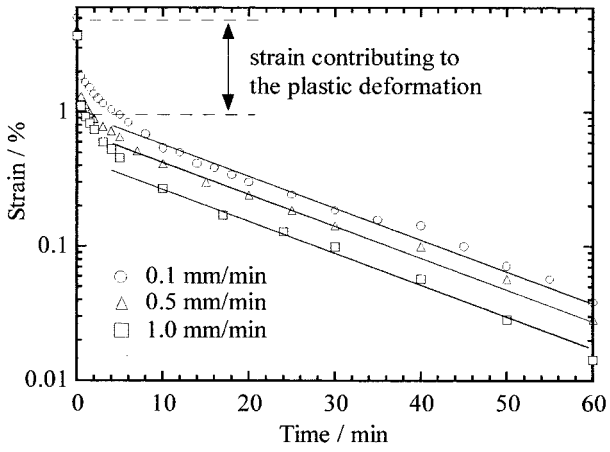

Figure 12 Semilogarithmic plots of the creep recovery curves. The solid lines are those fitted to eq. (8).

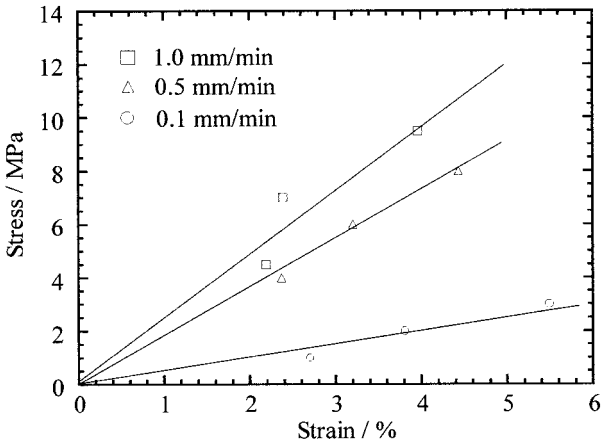

Figure 13 The relationship between the strain and the stress contributing to the plastic deformation.

Figures 13 and 14 show the stress and strain contributing to the plastic deformation as a function of strain applied to the samples, respectively. The stress contributing to the plastic deformation depends upon the applied strain, and the slope of the line increases with increasing strain rate. On the other hand, the strain in creep recovery curves depends upon the applied strain but is independent of the strain rate.

The plastic deformation for amorphous polymers in the glassy states is interpreted in terms of crazing and shear yielding.[13,18–20] The plastic deformation attributable to crazing is dominant for amorphous brittle polymers, such as PMMA. At the beginning of the deformation, microvoids are produced in the materials.[21–23] After the stress relaxation, while keeping the strain a constant, the residues of crazing will still remain in the materials, and the size or amount of the residues will depend upon the strain rate, as shown in Figure 13. However, the stress–strain relationship in state A depends upon the strain, but not on the strain rate, as is seen in Figure 4. In creep recovery process, strain rate dependence is no longer observable. It is difficult to detect the strain rate dependence from the stress–strain relationships in states A and B. On the other hand, the ultrasonic velocities of PMMA in states A and B not only depend upon the strain, but also the strain rate, as shown in Figure 8. The strain rate dependence of the ultrasonic velocities is related to that of the stress contributing to the plastic deformation. This result clearly indicates that the size or amount of the residues of crazing depends upon the strain rate and affects such mechanical properties as elasticity and compressibility.

The residues of crazing after stress or strain relaxation are not necessarily the same as the microvoids that are produced at an early stage of the plastic deformation. However, at this point, we consider them to be "microvoids." The ultrasonic velocity and adiabatic compressibility depend upon the quantity of microvoids. Thus, we can estimate the microvoids qualitatively by the following procedures.[2] If the additivity of compressibility for the volume fraction of microvoids holds, the adiabatic compressibility of PMMA deformed by the tensile stress is described as follows:

$$\beta = \phi_M \beta_M + \phi_P \beta_P \tag{9}$$

where ϕ is the volume fraction, and the subscripts M and P indicate microvoid and polymer, respectively. Assuming that the change of the adiabatic compressibility of polymer itself is small during the deformation, the adiabatic compressibility of virgin PMMA is used in the second term on the right-hand side of eq. (9). The adiabatic compressibility is calculated from the following relations:

$$\beta = 1/K \qquad K = M - (4/3)G \tag{10}$$

where K is the bulk modulus, M is the longitudinal modulus, and G is the shear modulus. The longitudinal modulus of PMMA deformed by the tensile stress was estimated from measured ultrasonic velocities and density data. The shear modulus of PMMA and the bulk modulus of mi-

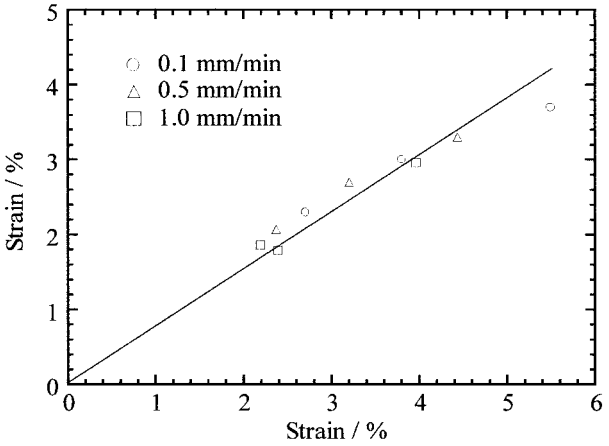

Figure 14 The relationship between the applied strain and the strain contributing to the plastic deformation. The abscissa represents the strain in state A.

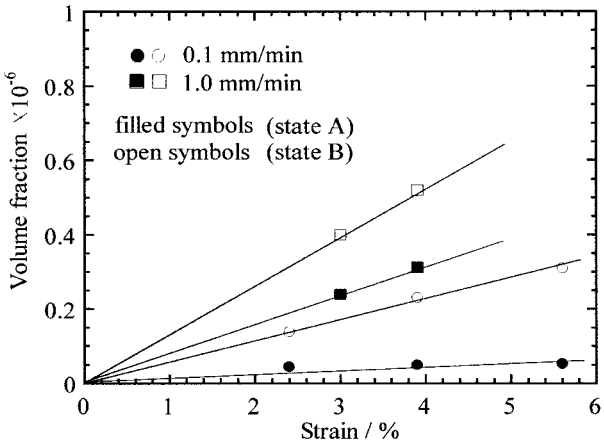

Figure 15 Strain dependence of the volume fraction of microvoids.

crovoids were estimated from the values found in the literature.[24] It is difficult to obtain the density data using conventional density measurements. The density of PMMA in state A is assumed to be equal to the value of virgin PMMA. The volume fraction of the microvoids estimated in this way is shown in Figure 15. The microvoid fraction is of the order of 10^{-7} and depends upon the testing conditions.[25] Precise density data of PMMA in state A is needed to investigate the difference between the volume fraction in states A and B.

As shown in Figure 9, the COBS measurements clearly demonstrated the single velocity dispersion in the frequency range of 100 MHz to 1 GHz, and its relaxation frequency was around 400 MHz at room temperature. This relaxation process can be assigned to the γ-relaxation of PMMA according to the dispersion map reported by Tanabe et al.[26] The γ-relaxation process of PMMA is attributed to the rotation of α-methyl groups in PMMA. The relaxation frequency and amplitude of the γ-relaxation were unaffected by the deformation processes. This means that even in the large deformation, amorphous part of polymeric materials is predominant, and local molecular motion of polymer chain does not affect the viscoelastic and also plastic deformations.

CONCLUSION

The acoustic properties of PMMA deformed by the tensile stress were studied by the COBS method. The COBS method has been successfully used to measure ultrasonic velocities of PMMA in different steady stress–strain states without contact with specimens. The major results obtained are summarized as follows. First, the ultrasonic velocities decreased with increasing the strain, and the ratio of the decrease increased with increasing the strain rate. This shows that the residues of crazing still remain in the steady stress–strain states, and the dimension or amount of the residues depends upon the strain rate. Second, the γ-relaxation of PMMA was observed around 400 MHz at room temperature. The relaxation frequency and amplitude of the γ-relaxation observed in the deformed PMMA were in agreement with those observed in virgin PMMA. The viscoelastic and plastic deformations have little effect on the γ-relaxation.

REFERENCES

1. Koda, S.; Yamashita, K.; Matsumoto, K.; Nomura, H. Japan J Appl Phys 1993, 32, 2234.
2. Koda, S.; Yamashita, K.; Iwai, S.; Nomura, H.; Iwata, M. Polymer 1994, 35, 5626.
3. Kumar, S. S.; Fartash, A.; Grimsditch, M.; Schuller, I. K.; Kumar, R. S. Macromolecules 1993, 26, 6184.
4. Forrest, J. A.; Rowat, A. C.; Dalnoki, V. K.; Stevens, J. R.; Dutcher, J. R. J Polym Sci (B) Polym Phys 1996, 34, 3009.
5. Yap, B. C.; Shichijyo, S.; Matsushige, K.; Takemura, T. Japan J Appl Phys 1982, 21, L523.
6. Kawabe, H.; Natsume, Y.; Higo, Y.; Nonomura, S. J Mat Sci 1992, 27, 5547.
7. Nielsen, L. E. Mechanical Properties of Polymers and Composites; Dekker: New York, 1974; Chapter 3.
8. Tanaka, H.; Sonehara, T.; Takagi, S. Phys Rev Lett 1997, 79, 881.
9. Sakurai, T.; Matsuoka, T.; Koda, S.; Nomura, H. J Acoust Soc Japan E 1998, 19, 297.
10. Sakurai, T.; Asai, M.; Matsuoka, T.; Koda, S.; Nomura, H. Japan J Appl Phys 1998, 37, 6098.
11. Sadd, M. H.; Morris, D. H. J Appl Polym Sci 1976, 20, 421.
12. Hattori, K.; Matsuoka, T.; Sakai, K.; Takagi, K. Japan J Appl Phys 1994, 33, 3217.
13. Williams, J. G. Fracture Mechanics of Polymers; Ellis Horwood: London, 1984.
14. Dibenedetto, A. T.; Trachte, K. L. J Appl Polym Sci 1970, 14, 2249.
15. Nicolais, L.; Dibenedetto, A. T. J Appl Polym Sci 1971, 15, 1585.

16. Flugge, W. Viscoelasticity; Blaisdell Publishing: Waltham Massachusetts, 1967.
17. Williams, J. G. Stress Analysis of Polymers; Longman Group Ltd: London, 1973.
18. Argon, A. S. Plastic deformation and fracture; VCH publisher: Weinheim, 1992.
19. Kramer, E. J. Adv Polym Sci 1983, 52/53, 1.
20. Kramer, E. J.; Berger, L. L. Adv Polym Sci 1990, 91/92, 1.
21. Bhan, P.; Devis, M.; Hull, D. J Mat Sci 1972, 8, 162.
22. Paredes, E.; Fisher, E. W. Macromol Chem 1979, 180, 2707.
23. Donald, A. M.; Kramer, E. J. Phil Mag 1981, A43, 857.
24. Handbook of Ultrasonic Technology; The Nikkan Kogyo Shimbun: Tokyo, 1966.
25. He, C.; Donald, A. M.; Butler, M. F. Macromolecules 1998, 31, 158.
26. Tanabe, Y.; Hirose, J.; Okano, K.; Wada, Y. Polym J 1970, 1, 107.